STIM1, an essential and conserved component of store-operated Ca^{2+} channel function

Jack Roos,[1] Paul J. DiGregorio,[1] Andriy V. Yeromin,[2] Kari Ohlsen,[1] Maria Lioudyno,[2] Shenyuan Zhang,[2] Olga Safrina,[2] J. Ashot Kozak,[2] Steven L. Wagner,[1] Michael D. Cahalan,[2] Gönül Veliçelebi,[1] and Kenneth A. Stauderman[1]

[1]Torrey Pines Therapeutics, Inc., La Jolla, CA 92037
[2]Department of Physiology and Biophysics and Center for Immunology, University of California, Irvine, CA 92697

Store-operated Ca^{2+} (SOC) channels regulate many cellular processes, but the underlying molecular components are not well defined. Using an RNA interference (RNAi)-based screen to identify genes that alter thapsigargin (TG)-dependent Ca^{2+} entry, we discovered a required and conserved role of *Stim* in SOC influx. RNAi-mediated knockdown of *Stim* in *Drosophila* S2 cells significantly reduced TG-dependent Ca^{2+} entry. Patch-clamp recording revealed nearly complete suppression of the *Drosophila* Ca^{2+} release-activated Ca^{2+} (CRAC) current that has biophysical characteristics similar to CRAC current in human T cells. Similarly, knockdown of the human homologue STIM1 significantly reduced CRAC channel activity in Jurkat T cells. RNAi-mediated knockdown of STIM1 inhibited TG- or agonist-dependent Ca^{2+} entry in HEK293 or SH-SY5Y cells. Conversely, overexpression of STIM1 in HEK293 cells modestly enhanced TG-induced Ca^{2+} entry. We propose that STIM1, a ubiquitously expressed protein that is conserved from *Drosophila* to mammalian cells, plays an essential role in SOC influx and may be a common component of SOC and CRAC channels.

Introduction

Store-operated Ca^{2+} (SOC) influx is an important process in cellular physiology that controls such diverse functions as refilling of intracellular Ca^{2+} stores (Putney and Bird, 1993), activation of enzymatic activity (Fagan et al., 2000), gene transcription (Lewis, 2001), and release of cytokines (Winslow et al., 2003). In T lymphocytes and mast cells, SOC influx occurs through Ca^{2+} release-activated Ca^{2+} (CRAC) channels, a type of SOC channel that has been characterized extensively in patch-clamp experiments. Although considerable work has focused on the process of SOC entry and the biophysical properties of CRAC channels, the molecular components of the underlying channels and the mechanisms controlling them are still unclear (Lewis, 2001; Venkatachalam et al., 2002; Prakriya and Lewis, 2003). We recently characterized a store-operated Ca^{2+}-selective current in *Drosophila* S2 cells and showed that it shares many of the properties of CRAC current in mammalian immune cells (Yeromin et al., 2004). *Drosophila* S2 cells, believed to be of hematopoietic origin (Towers and Sattelle, 2002), may provide an advantage over many other cell types in studying CRAC channel function because S2 cells lack contaminating currents from other channel types (Yeromin et al., 2004). Furthermore, these cells are particularly useful for gene silencing experiments, as they display highly efficient RNA interference (RNAi) with relatively simple protocols (Clemens et al., 2000; Worby et al., 2001). Thus, S2 cells are an appropriate model system to test the role of candidate genes in SOC influx using RNAi.

Several gene products have been proposed to play a role in SOC influx. For example, at the level of the plasma membrane a number of studies have suggested that a subset of TRP proteins might be responsible for SOC influx (for reviews see Clapham, 2003; Montell, 2003). However, SOC channels exhibit varying biophysical properties depending on cell type and it remains unclear which proteins may be involved in forming the channel or regulating channel activation (Prakriya and Lewis, 2003). In mammalian cells, TRPC1 (Mori et al., 2002), TRPC3 (Philipp et al., 2003), TRPC4 (Philipp et al., 2000; Tiruppathi et al., 2002), and TRPV6 (CaT1; Yue et al., 2001; Cui et al., 2002; Schindl et al., 2002) have been proposed to underlie SOC influx or channel activity, but these identifications remain controversial (Voets et al., 2001; Prakriya and Lewis, 2003; Kahr et al., 2004).

A.V. Yeromin and P.J. DiGregorio contributed equally to this work.

Correspondence to K.A. Stauderman: kstauderman@torreypinestherapeutics.com; or M.D. Cahalan: mcahalan@uci.edu

Abbreviations used in this paper: $[Ca^{2+}]_i$, intracellular free Ca^{2+} concentration; CRAC, Ca^{2+} release-activated Ca^{2+}; dsRNA, double-stranded RNA; $iPLA_2$, Ca^{2+}-independent PLA_2; RFU, relative fluorescence unit; RNAi, RNA interference; SOC, store-operated Ca^{2+}; SOCE, SOC entry; TG, thapsigargin.

The online version of this article contains supplemental material.

The Journal of Cell Biology, Vol. 169, No. 3, May 9, 2005 435–445
http://www.jcb.org/cgi/doi/10.1083/jcb.200502019

We sought to identify new genes potentially involved in SOC influx in a more systematic fashion. To accomplish this, an experimental system using *Drosophila* S2 cells was developed in which expression of several targeted gene products were individually suppressed by RNAi and evaluated for their role in SOC influx. S2 cells express a thapsigargin (TG)-sensitive SERCA pump that serves to fill an intracellular store linked to the activation of SOC influx (Magyar and Varadi, 1990; Vazquez-Martinez et al., 2003). TG-induced Ca^{2+} entry in S2 cells has been demonstrated by fura-2 ratiometric techniques (Yagodin et al., 1999). We now report the identification of *Stim* as a critical component of TG-dependent Ca^{2+} influx and CRAC channel function in S2 cells. *Stim* is a type I transmembrane protein with two mammalian homologues, STIM1 and STIM2. We further demonstrate that the ubiquitously expressed homologue STIM1 controls CRAC channel function in human Jurkat T cells. Finally, we show that STIM1, but not STIM2, regulates SOC influx in human cells. STIM1 thus represents a conserved component regulating SOC influx and CRAC channel activity.

Results

Screening for genes that regulate SOC influx in *Drosophila* S2 cells: identification of CG9126 (*Stim*)

To examine the role of individual target genes in SOC influx, a 96-well plate fluorescence assay was used to detect changes in intracellular free Ca^{2+} concentration ($[Ca^{2+}]_i$) evoked by TG in conjunction with RNAi. Selected to include channel-like domains, transmembrane regions, Ca^{2+}-binding domains, or putative function in SOC influx, 170 genes were tested for involvement in Ca^{2+} signaling by incubating S2 cells with double-stranded RNA (dsRNA) corresponding to 500 bp fragments of the candidate genes (Table S1, available at http://www.jcb.org/cgi/content/full/jcb.200502019/DC1). Control S2 cells displayed both TG-independent and TG-dependent Ca^{2+} influx (Fig. 1 A). The TG-dependent Ca^{2+} response reached a plateau within three minutes of re-adding external Ca^{2+}, and was inhibited by 20 μM 2-APB (Fig. 1 B) or 50 μM SKF96365 (not depicted), which is consistent with the block of *Drosophila* CRAC currents by these compounds (Yeromin et al., 2004). These results suggest that the TG-dependent SOC influx signal reflects activity of the *Drosophila* CRAC channel. Cells incubated with a dsRNA probe to gene CG9126 (*Drosophila Stim*) displayed TG-dependent Ca^{2+} entry that was reduced by >90% compared with control, whereas the TG-independent Ca^{2+} signal was reduced by only 10% (Fig. 1 C). In parallel, the level of *Stim* mRNA was reduced by >50% compared with control (Fig. 1 D). A separate dsRNA targeting a different region of *Stim* (see Materials and methods) produced equivalent suppression of the SOC influx signal (unpublished data). Finally, suppression of *Stim* did not alter growth rate or loading with fluo-4, which is consistent with healthy cells.

Stim is annotated in FlyBase as a cell adhesion molecule, presumably based upon studies first identifying its mammalian homologue STIM1 in a screen for cell adhesion molecules (Oritani and Kincade, 1996). Although we did not observe any morphological or cell attachment effects in *Stim*-knockdown cells, we examined effects of RNAi directed at six genes that are annotated as scaffolding or cell adhesion genes (Table S1;

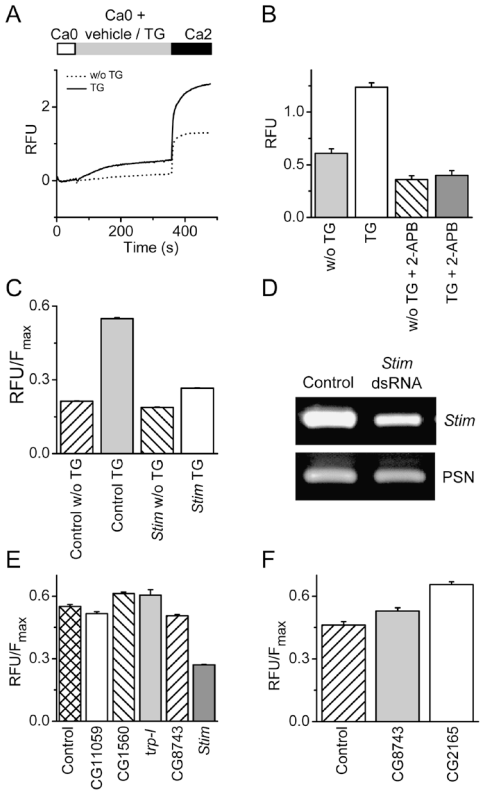

Figure 1. **Essential role of gene CG9126 (*Stim*) in SOC influx in *Drosophila* S2 cells.** (A) *Drosophila* SOC influx measured in a fluorimeter. Basal-subtracted fluo-4 fluorescence in relative fluorescence units (RFUs) from *Drosophila* S2 cells in a 96-well plate. Cells were initially in Ca^{2+}-free solution (Ca0). Bars indicate addition of TG (1 μM, solid line) or vehicle (dotted line), followed by 2 mM Ca^{2+} (Ca2). The TG-independent response can be explained by partial store depletion during exposure to Ca^{2+}-free solution or possible damage to some cells. Traces are averages of recordings from four individual wells. (B) Development of an end point assay for screening gene candidates. Cells were treated as described in A and placed in a fluorimeter 3 min after adding 2 mM Ca^{2+}. Pre-incubating cells with 20 μM 2-APB reduced TG-dependent Ca^{2+} entry significantly ($P < 5 \times 10^{-6}$: unpaired *t* test) and to a greater extent than the TG-independent Ca^{2+} entry ($P < 5 \times 10^{-6}$: unpaired *t* test); $n = 24$ for each treatment group. (C) Treatment of *Drosophila* S2 cells with *Stim* dsRNA inhibits SOC influx by 90% ($P < 10^{-5}$; unpaired *t* test compared with control mock-treated cells). Data represent basal-subtracted RFUs divided by maximal fluorescence (F_{max}) to normalize for cell number. The TG-dependent Ca^{2+} signal can be obtained by subtracting the average TG-independent signal from the Ca^{2+} signal after treatment with TG. Knockdown of *Stim* also inhibited the TG-independent Ca^{2+} signal (vehicle) by <10%, albeit significantly ($P < 10^{-4}$, unpaired *t* test). (D) mRNA reduction in *Stim* dsRNA-treated cells. RNA was isolated from mock-treated cells or cells treated with a dsRNA specific to *Stim*. RT-PCR analysis was performed using gene-specific primers to *Stim* or to a control gene, presenilin (PSN). (E) Suppression of other candidate genes did not markedly inhibit TG-induced Ca^{2+} influx. Cells were mock treated or treated with dsRNA specific for CG11059, CG1560, *trp-l*, CG8743, or *Stim* for 5 d. Ca^{2+} influx was measured after pretreatment with TG. Data represent basal-subtracted RFUs divided by F_{max} to normalize for cell number. (F) Knockdown of CG8743 or CG2165 elevates basal intracellular Ca^{2+} levels. Cells were mock treated (control) or treated with dsRNA specific for CG8743 or CG2165 for 5 d. Data represents basal RFUs divided by the maximum fluorescence, F_{max}, to normalize to cell number ($P < 0.01$, one-way ANOVA, Dunnett's multiple comparison test compared with control mock-treated cells). (B, C, E, and F) Error bars represent means ± SD.

CG11324, CG3504, CG11059, CG1560, CG5723, CG6378). Except for *Stim*, none of the cell adhesion molecules tested had a significant effect on TG-dependent Ca^{2+} entry (Fig. 1 E). The role of TRP-family proteins as molecular candidates for the CRAC channel has been widely discussed (Clapham, 2003; Montell, 2003). To test the possible role of *trp*-related proteins in S2 cells, we treated cells with dsRNAs corresponding to every known *Drosophila trp* gene (*trp*, *trp-l*, and *trp-gamma*) or *trp*-related gene (TRPM-type, CG16805; TRPV-type, CG5842, CG4536; TRPML-type, CG8743; TRPN-type, CG11020 (*nompC*); TRPA-type, CG15860 (*painless*), CG5751, CG17142, CG10409; and TRPP-type, CG6504) identified in silico, regardless of whether expression in S2 cells could be verified by RT-PCR (Table S1). Additionally, we treated cells with a pool of dsRNAs corresponding to *trp*, *trp-l*, and *trp-gamma*. In no instance were we able to measure an effect on SOC influx, despite confirming suppression of corresponding mRNAs (Table S1). When targeted by RNAi, two genes, CG2165 (the *Drosophila* homologue of the plasma membrane-Ca^{2+}-ATPase) and CG8743 resulted in an elevation of basal intracellular Ca^{2+} levels (Fig. 1 F). However, neither CG2165 nor CG8743 had an effect on TG-dependent SOC influx. Of 170 genes with a potential role in SOC influx, only *Drosophila Stim* demonstrated a major effect on SOC entry (SOCE) when suppressed by RNAi.

Suppression of TG-dependent Ca^{2+} influx in individual S2 cells by *Stim* dsRNA

Population measurements of intracellular Ca^{2+} would include contributions of cells that had not been affected by gene silencing. Therefore, to clarify effects of gene silencing at the level of single cells we evaluated Ca^{2+} signaling and CRAC currents in S2 cells that were pretreated with dsRNA. Fig. 2 A illustrates Ca^{2+} signals in response to TG-evoked store depletion in eight individual control cells treated with dsRNA for the cell adhesion molecule CG1560. Removal of Ca^{2+} and readdition of Ca^{2+} produced no significant change in the Ca^{2+} signal. Addition of TG in zero-Ca^{2+} solution produced a transient rise in $[Ca^{2+}]_i$ due to release of Ca^{2+} from the ER; the release transient reached a peak that averaged ~200 nM before declining. Upon readdition of Ca^{2+}, store-operated Ca^{2+} influx was revealed as a rise in $[Ca^{2+}]_i$ that was sustained and often exceeded 1 μM. In cells that were pretreated with *Stim* dsRNA, resting $[Ca^{2+}]_i$ and the release transient were not altered significantly, but the rise in Ca^{2+} upon readdition of external Ca^{2+} was prevented in most of the single cells (Fig. 2 B). In contrast, suppression of CG8743 produced a significant elevation of the resting $[Ca^{2+}]_i$ to ~60% higher than in control cells (135 CG1560 dsRNA-treated control cells; 118 CG8743 dsRNA-treated cells; $P < 5 \times 10^{-6}$), which is consistent with results from the initial screen (Fig. 1 F). However, CG8743 dsRNA did not alter the Ca^{2+}-release transient (not depicted) or Ca^{2+} influx evoked by TG (Fig. 1 E). Fig. 2 C summarizes the results of three control experiments and six experiments with suppression of *Stim*. Occasionally, cells in the *Stim* dsRNA group exhibited normal Ca^{2+} responses similar to control cells, suggesting either that these cells did not effectively take up the dsRNA, that gene

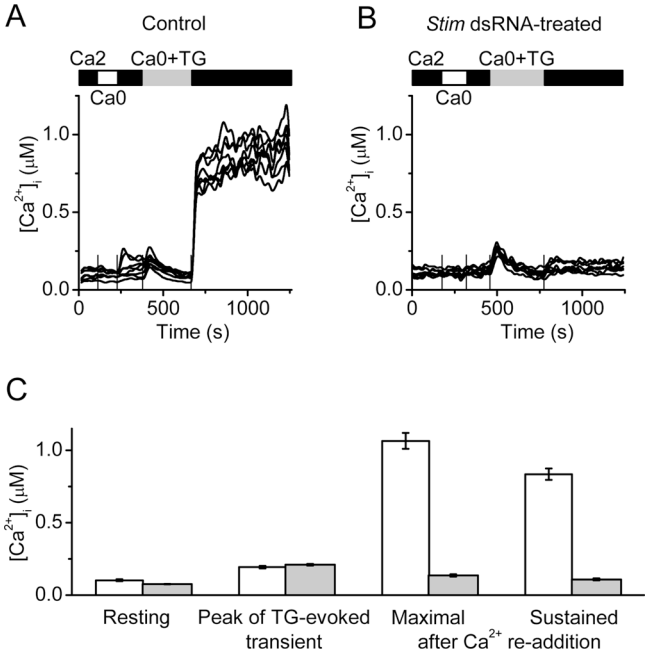

Figure 2. **Suppression of Ca^{2+} signal by *Stim* dsRNA treatment.** (A) $[Ca^{2+}]_i$ in single cells treated with CG1560 dsRNA (control). Solution exchanges are indicated by solid (S2 Ringer with 2 mM Ca^{2+}), open (Ca^{2+} free), and gray (Ca^{2+}-free containing 1 μM TG) bars, respectively. Vertical lines indicate the time of solution exchange. (B) Intracellular Ca^{2+} responses in S2 cells treated with *Stim* dsRNA. (C) Averaged values ± SEM for control cells ($n = 46$ cells in two representative experiments, white bars) and *Stim* dsRNA-treated ($n = 197$ cells in three representative experiments, gray bars): resting $[Ca^{2+}]_i$; peak $[Ca^{2+}]_i$ during the TG-evoked release transient; maximal and sustained (5 min) $[Ca^{2+}]_i$ after readdition of 2 mM external Ca^{2+}. The values of maximal $[Ca^{2+}]_i$ and sustained $[Ca^{2+}]_i$ in control and *Stim* suppressed cells are significantly different ($P < 5 \times 10^{-6}$).

suppression in these cells was less efficient, or that some cells with effective gene suppression express normal SOC influx, as found in DT40 cells after knockout of TRPC1 (Mori et al., 2002). These results demonstrate at the single-cell level that suppression of *Stim* effectively blocks both the early and sustained components of Ca^{2+} entry evoked by TG.

Suppression of *Drosophila* CRAC current by *Stim* dsRNA

In previous work, we demonstrated that Ca^{2+} entry evoked in S2 cells by Ca^{2+} store depletion occurs through store-operated Ca^{2+}-selective channels that are similar in biophysical properties to CRAC channels in T lymphocytes (Yeromin et al., 2004). Fig. 3 (A and B) illustrates the time course of CRAC current development and the characteristic I-V relationship in control cells dialyzed with the Ca^{2+} chelator BAPTA to deplete Ca^{2+} stores passively. In cells treated with dsRNA for *Stim*, CRAC current was effectively suppressed in most cells (Fig. 3, C and D). We performed similar experiments on six groups of cells: control cells that were untreated; two additional control groups in which cells were treated with dsRNA for cell adhesion molecules CG11059 and CG1560; cells treated with dsRNA directed against two *trp*-related genes that are expressed in S2 cells, *trp-l* and CG8743; or cells treated with dsRNA for *Stim*. Suppression of corresponding gene expression was confirmed by RT-PCR

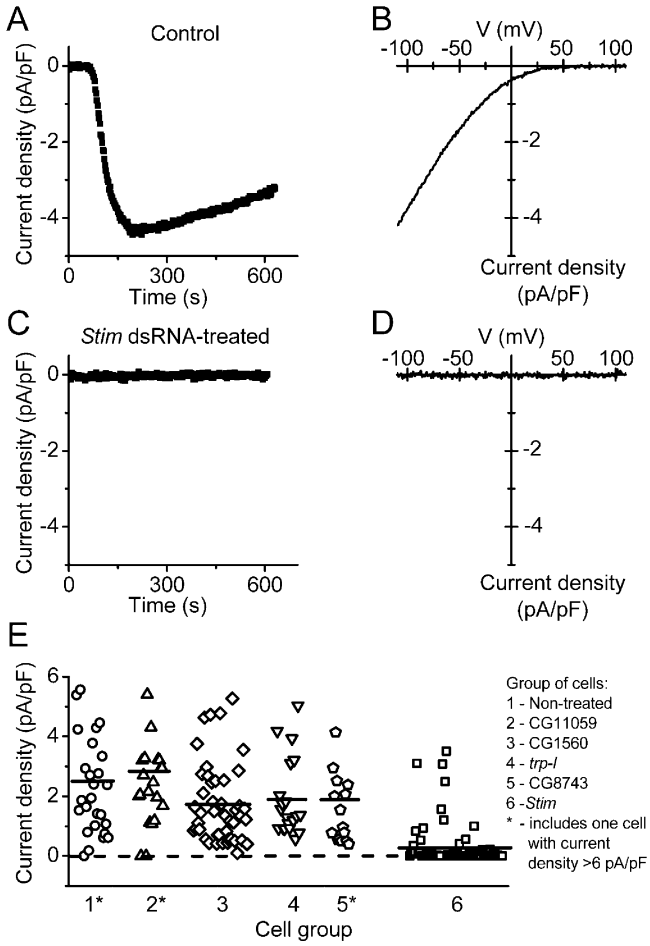

Figure 3. **Suppression of *Drosophila* CRAC current by *Stim* dsRNA treatment.** (A) Current development evaluated at −110 mV in selected control cell (untreated). Cells were bathed in S2 external solution with 2 mM Ca^{2+} and dialyzed with BAPTA-buffered S2 internal solution to induce store depletion passively. Whole-cell recording was initiated at time 0. (B) Leak-subtracted current-voltage relation of maximal *Drosophila* CRAC current recorded in the same control cell. (C) Typical *Stim* dsRNA-treated cell; current at −110 mV. (D) Leak-subtracted I-V relation 200 s after establishing the whole cell configuration. (E) CRAC current density in dsRNA-treated and untreated S2 cells. Each point represents CRAC current density (pA/pF) in a single cell, plotted in consecutive order from left to right within six groups of cells: untreated (circles, $n = 27$ cells in three experiments); cells treated with dsRNA to suppress CG11059 (triangles, $n = 21$ cells in three experiments); CG1560 (diamonds, $n = 45$ cells in six experiments); *trp-l* (inverted triangles, $n = 20$ cells in two experiments); CG8743 (pentahedrons, $n = 16$ cells in two experiments); or *Stim* (squares, $n = 77$ cells in eight experiments). Groups 1, 2, and 5 include one cell each with current density >6 pA/pF. Horizontal lines indicate the mean value of current density in each group.

(unpublished data). As summarized in Fig. 3 E, CRAC currents were similar in all three control groups and in the *trp-l* and CG8743-suppressed groups. In the *Stim* dsRNA-treated cells, CRAC currents were suppressed to undetectable levels in 83% of cells. These experiments demonstrate that *Drosophila Stim* is required for normal activity of CRAC channels in S2 cells.

Inhibition of Ca^{2+} entry in STIM1-suppressed Jurkat T cells

Mammalian cells express two homologues, STIM1 and STIM2, of *Drosophila Stim*. Both are single-pass transmembrane proteins that are present in rat, mouse, and human. STIM1 was detected by Western blot in human Jurkat T cells (Fig. 4 A) and in primary human T lymphocytes (not depicted). In these cells, T cell receptor stimulation leads to activation of the CRAC channel and subsequent gene expression and cytokine release (Lewis, 2001). To test the role of STIM1 in T cells, a stable pool of Jurkat cells expressing a short RNA hairpin loop (shRNA) targeting human STIM1 was generated (Jurkat clone 4A5). Stable pools of Jurkat cells expressing a negative control, nonsilencing scrambled shRNA were also generated (Jurkat negative control clone 2A4). In these cells, STIM1 mRNA and protein were reduced by >50%, but there was no change in STIM2 mRNA levels indicating specificity of the STIM1 shRNA (Fig. 4, A and B). Importantly, TG-dependent Ca^{2+} influx was significantly reduced in the 4A5 Jurkat cells, as seen in individual cells and the averaged responses (Fig. 4, C–G). Removal and readdition of Ca^{2+} produced no significant change in the Ca^{2+} signal, indicating that the TG–independent response was negligible (unpublished data). TG-dependent Ca^{2+} influx rates were evaluated from the maximal rate of rise in the Ca^{2+} signal, $d[Ca^{2+}]_i/dt$, upon Ca^{2+} readdition in both Jurkat Ringer and low-Ca^{2+} Jurkat Ringer (Fig. 4, H and I); STIM1 suppression reduced mean influx rates by 68% and 82%, respectively. These results confirm that Ca^{2+} influx in Jurkat T cells is effectively inhibited by suppression of STIM1, as seen for *Stim* in S2 cells.

CRAC current reduction by STIM1 suppression in individual Jurkat T cells

Depletion of Ca^{2+} stores in Jurkat T cells leads to the opening of CRAC channels that can be monitored as CRAC current (Prakriya and Lewis, 2003). STIM1 suppression in 4A5 Jurkat T cells reduced the average CRAC current density evaluated during whole-cell recording. The time course of current and corresponding I-V relations recorded from one control and one STIM1-suppressed cell are shown in Fig. 5 (A–D), and a summary of data is presented in Fig. 5 E. Only ~9% of STIM1-suppressed cells developed detectable current, compared with 70% of control cells. In cells that exhibited detectable CRAC current, the inactivating Na^+ current through CRAC channels upon exposure to divalent-free external solution was also reduced. The ratio of peak Na^+ to Ca^{2+} current was similar in control 2A4 cells (10 ± 1.4, $n = 6$) and in STIM1-suppressed cells 4A5 cells (12.2 ± 2.8, $n = 5$). The attenuation of CRAC currents in Jurkat T cells is consistent with Ca^{2+} imaging results described above.

STIM1 modulates SOCE in mammalian cells

To further examine the role of STIM1 in SOCE in mammalian cells, we generated siRNAs to STIM1 and STIM2 and tested them individually in HEK293 cells on TG-induced Ca^{2+} influx, previously linked to TRPC1 and TRPC3 proteins (Wu et al., 2000). RT-PCR and Western blot analysis indicated that STIM1 mRNA and protein levels were selectively reduced by the STIM1 siRNA (Fig. 6, A and B). Immunofluorescence lo-

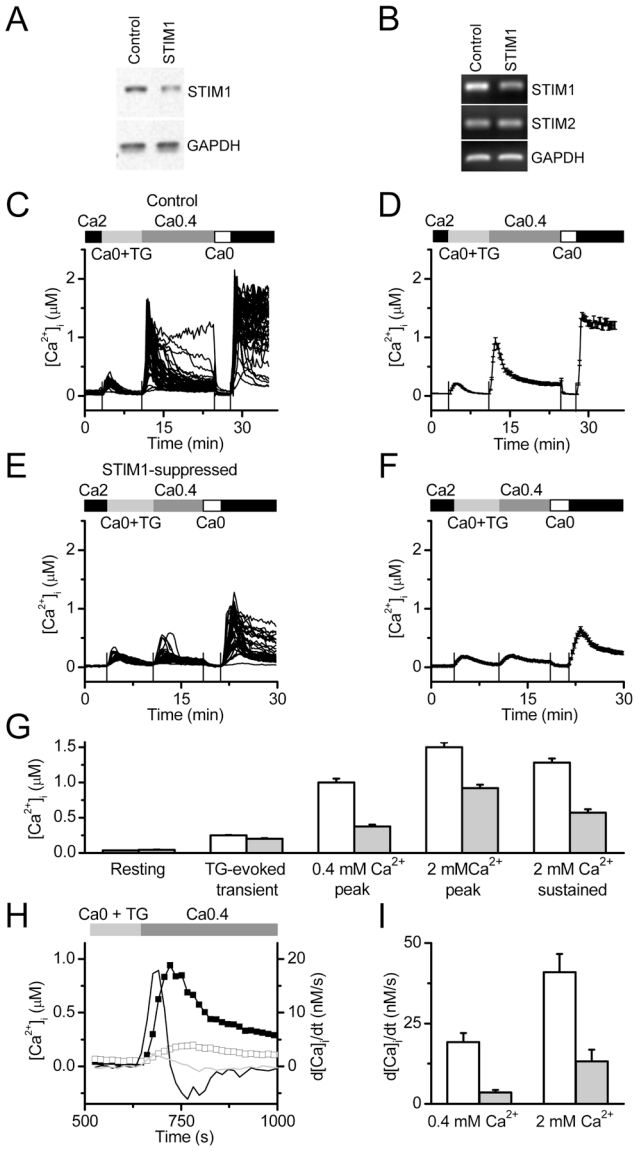

Figure 4. **The effect of STIM1 suppression on Ca^{2+} signaling in individual Jurkat T cells.** (A) Western blot of 4A5 cell lysates (lane 2), compared with control 2A4 cells (lane 1) showing >50% reduction in STIM1 protein, with no change in the protein levels of GAPDH. (B) The specificity of STIM1 suppression was confirmed by RT-PCR analysis showing a reduction in STIM1, but not STIM2 or GAPDH, mRNA levels in 4A5 cells (lane 2) compared with control 2A4 cells (lane 1). (C) Intracellular Ca^{2+} responses in 51 Jurkat 2A4 control cells. Cells were bathed in Jurkat Ringer (2 mM Ca^{2+}), low-Ca^{2+} (0.4 mM) Jurkat Ringer, and Ca^{2+}-free Jurkat Ringer with 1 μM TG, as indicated. The first peak is due to Ca^{2+} release from internal stores in the presence of TG. The second and third peaks result from Ca^{2+} entry through CRAC channels upon addition of 0.4 and 2 mM external Ca^{2+}, respectively. Sustained $[Ca^{2+}]_i$ was measured 5 min after readdition of 2 mM external Ca^{2+}. (D) Averaged $[Ca^{2+}]_i$ in control 2A4 cells from the same experiment. (E) Intracellular Ca^{2+} responses in 40 STIM1-suppressed 4A5 Jurkat cells. (F) Averaged $[Ca^{2+}]_i$ in STIM1-suppressed 4A5 cells from the same experiment as in D. (G) Combined data from three control experiments (164 cells, white bars) and three experiments with STIM1-suppressed cells (141 cells, gray bars). Averaged values of peak and sustained $[Ca^{2+}]_i$ are significantly different in STIM1-suppressed cells ($P < 8 \times 10^{-6}$, $< 8 \times 10^{-6}$, and $< 2 \times 10^{-5}$, respectively, by independent two populations *t* test). (H) Maximal rate of Ca^{2+} rise upon Ca^{2+} readdition as an estimate of Ca^{2+} influx. Representative averaged traces obtained in the same experiments as in A–D are shown (control 2A4 cells, closed squares; STIM1-suppressed 4A5 cells, open squares), along with corresponding differentiated $[Ca^{2+}]_i$ traces, $d[Ca^{2+}]_i/dt$ (right axis), for control 2A4 cells (black line without symbols) and STIM1-suppressed 4A5 cells (gray line). The peak derivatives correspond to the maximal rate of Ca^{2+} rise in nM. (I) STIM1 expression and $d[Ca^{2+}]_i/dt$. The maximal rate of $[Ca^{2+}]_i$ rise after 0.4 mM or 2 mM Ca^{2+} readdition in control 2A4 cells (white bars: 164 cells in three experiments); and STIM1-suppressed 4A5 cells (gray bars: 141 cells in three experiments; $P < 3 \times 10^{-7}$ or $< 2 \times 10^{-7}$ for 0.4 and 2 mM Ca^{2+}, respectively).

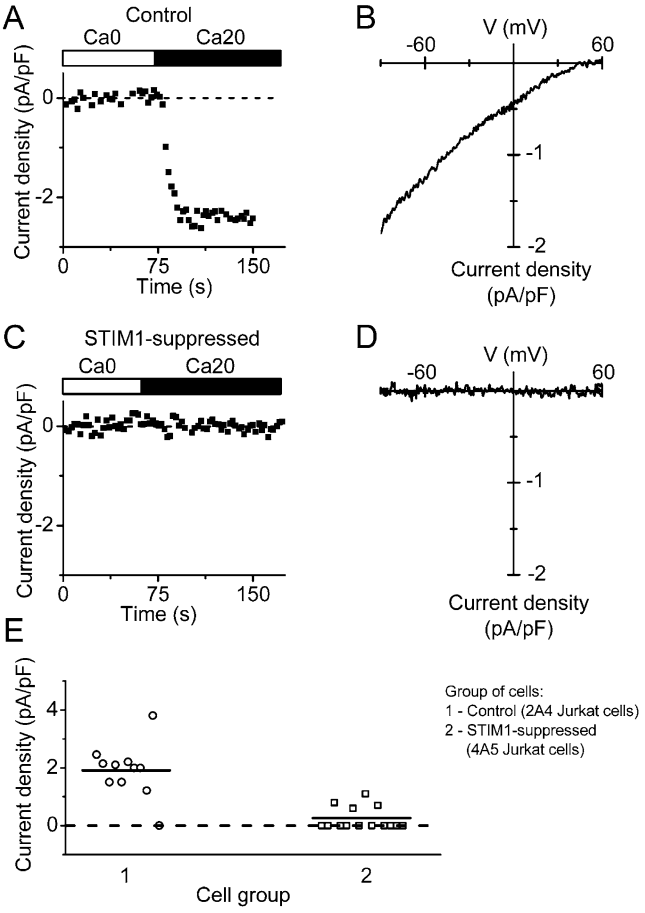

Figure 5. **Reduction of Jurkat CRAC current by STIM1 suppression.** (A) Current development in selected control 2A4 Jurkat cell. Cells were first bathed in Ca^{2+}-free Jurkat external solution for 5 min and dialyzed with BAPTA-containing Jurkat internal solution. CRAC current was revealed after exchange of Ca^{2+}-free Jurkat solution to 20 mM Ca^{2+} Jurkat external solution. Maximal current density was evaluated at −110 mV. (B) Leak-subtracted current-voltage relationship of fully developed CRAC current recorded in the same control 2A4 Jurkat cell. (C) Suppression of CRAC current in STIM1-suppressed 4A5 Jurkat cell. (D) Leak-subtracted I-V relationship in the same cell, as in C. (E) CRAC current density in control 2A4 cells (circles, $n = 11$) and STIM1-suppressed 4A5 cells (squares, $n = 11$). Horizontal lines indicate the mean value of current density in each group. ($P < 3 \times 10^{-6}$).

calization indicated an expression pattern consistent with plasma membrane and ER localization (Manji et al., 2000) and confirmed the reduction of STIM1 protein by RNAi (Fig. 6 C). Cellular metabolism of the mitochondrial substrate alamarBlue was not altered (unpublished data), indicating the absence of cytotoxicity or mitochondrial stress after STIM1 suppression. In STIM1-suppressed cells, TG-dependent Ca^{2+} influx was inhibited by 60%, whereas the Ca^{2+} release transient was unaffected compared with control cells transfected with a nonsi-

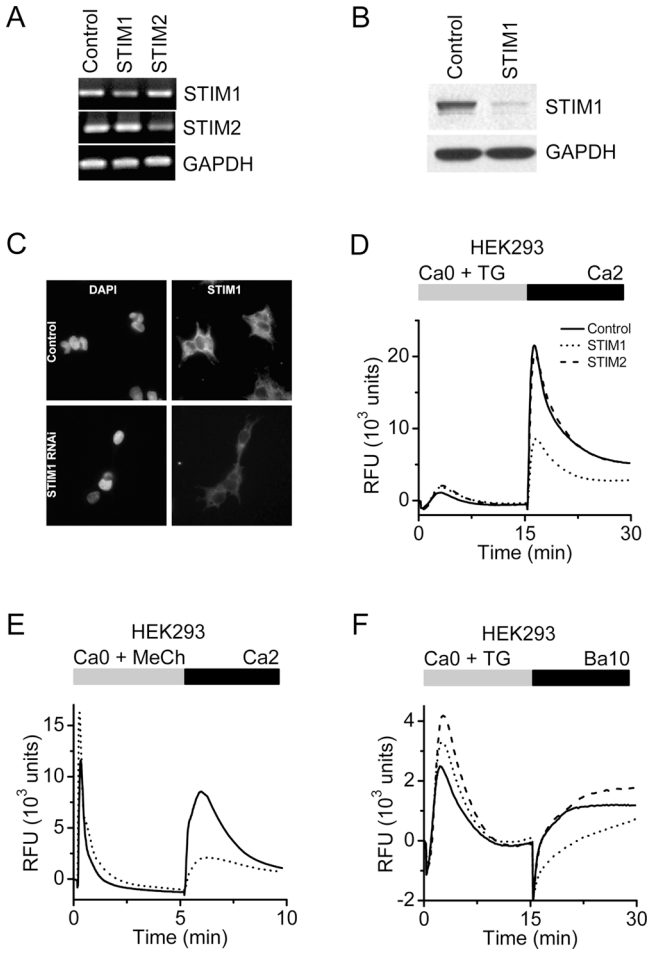

Figure 6. **Suppression of STIM1 in HEK293 cells inhibits SOC influx.** (A) RT-PCR analysis. STIM1 and STIM2 mRNA levels were reduced in cells transfected with the appropriate siRNA to <50% of control cells (transfected with scrambled siRNA). GAPDH levels were unchanged in either treatment group. (B) Western blot analysis. In cells transfected with the STIM1 siRNA, STIM1 protein levels were reduced to <10% of control levels, whereas GAPDH levels were unchanged. (C) Immunofluorescence localization of STIM1 in HEK293 cells. Nuclear staining pattern (left) with DAPI (Molecular Probes) in HEK293 cells treated with either a scrambled siRNA (top) or siRNA to STIM1 (bottom). No change in nuclear staining pattern or intensity was observed after RNAi-induced suppression of STIM1. STIM1-associated immunofluorescence (right) in HEK293 cells treated with either control (top) or STIM1 (bottom) siRNAs. In control cells, STIM1 has a diffuse reticulated localization pattern with some punctuate staining, which is consistent with expression associated with plasma membrane and ER. The intensity of STIM1 immunofluorescence was markedly decreased in the cells treated with STIM1 siRNA. (D) Calcium signals in HEK293 cells after RNAi-mediated knockdown. Suppression of STIM1 (dotted line) reduced SOC influx by 60% compared with control (solid line; $P < 10^{-4}$, unpaired *t* test), whereas suppression of STIM2 (dashed line) had little effect. Data indicate RFUs in 384-well plates monitored in a FLIPR^{384} fluorimeter. The traces are from a representative experiment, and are averaged signals from 48 wells per group. Traces from cells treated with vehicle (DMSO) instead of TG were essentially flat (not depicted for clarity). (E) Calcium signals after muscarinic receptor activation. RT-PCR analysis revealed that the muscarinic receptor, subtype m3, is expressed in our HEK293 cells (not depicted). 300 μM of methylcholine evoked Ca^{2+}-release transients in Ca^{2+}-free buffer were not inhibited by STIM1 suppression, but SOC influx upon readdition of 2 mM Ca^{2+} was greatly reduced in STIM1 siRNA-treated cells (dotted line) compared with control cells (solid line). The apparent enhancement of the methylcholine-evoked Ca^{2+} release transient in the STIM1-suppressed cells was not a consistent finding. (F) TG-induced Ba^{2+} entry. The rate of TG-induced Ba^{2+} entry in STIM1-suppressed cells (dotted line) was significantly lower than in control cells (solid line) or STIM2-suppressed cells (dashed line; $P < 10^{-4}$, unpaired *t* test).

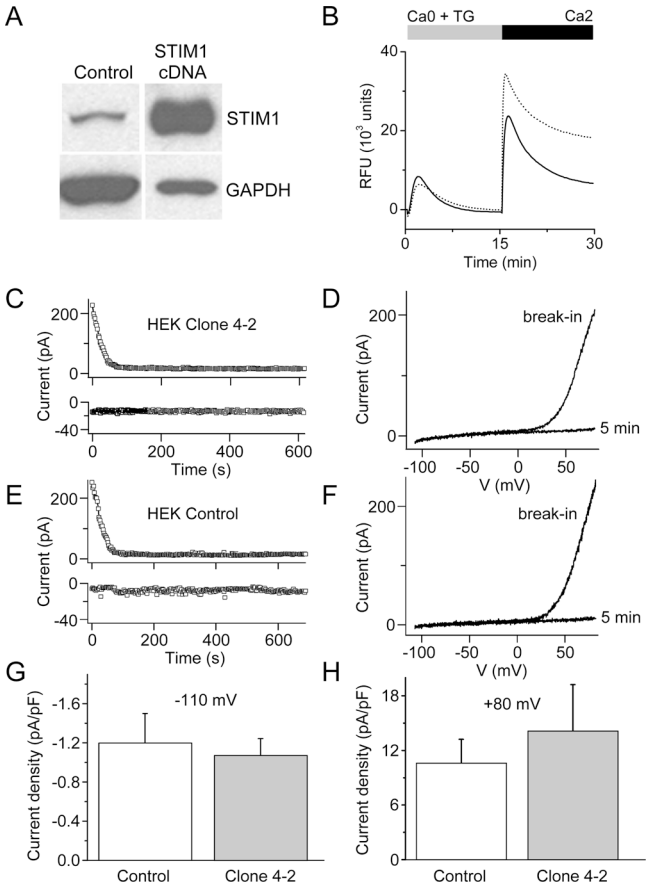

Figure 7. **Overexpression of STIM1 in HEK293 cells.** (A) Western blot analysis of STIM1 (top band) and GAPDH (bottom band) proteins in HEK-STIM1 (STIM1 overexpressing) cells and control cells (HEK-Zeo cells); lane 1, 10 μg protein; lane 2, 1 μg protein. We estimate STIM1 protein levels to be nearly 100-fold greater than in the HEK-STIM1 cells compared with control cells. (B) Representative traces of TG-induced Ca^{2+} release and TG-induced Ca^{2+} entry in HEK-STIM1 cells (dotted line) compared with HEK-Zeo cells (solid line). TG-induced Ca^{2+} entry was enhanced in HEK-STIM1 cells by an average of 17% in four experiments. (C and E) Time course of outward current at +80 mV and inward current at −110 mV (note different scales) for control HEK-Zeo (E) and HEK-STIM1 cells (C). (D and F) Representative current-voltage relationships immediately after break-in to achieve whole-cell recording and 5 min later in control HEK-Zeo (D) and HEK-STIM1 cells (F). Outwardly rectifying Mg^{2+}-inhibited cation current representing channel activity of TRPM7 disappeared as Mg^{2+} diffused into the cell from the pipette. (G and H) Inward and outward currents were not significantly altered by overexpression of STIM1; $n = 10$ cells for each group. Error bars represent SEM.

lencing scrambled siRNA (Fig. 6 D). In contrast, Ca^{2+} influx was unaltered in cells treated with the siRNA for STIM2, even though STIM2 mRNA was effectively reduced. In addition to inhibiting TG-evoked Ca^{2+} influx, knockdown of STIM1 potently inhibited muscarinic receptor-induced Ca^{2+} influx, but did not reduce IP_3-induced Ca^{2+} release (Fig. 6 E). The store-operated cation entry pathway in HEK293 cells is known to be permeable to Ba^{2+} (Wu et al., 2000; Trebak et al., 2002). Measurement of Ba^{2+} influx has the advantage of being a more direct reflection of cation entry via the plasma membrane because it avoids possible effects on cellular buffering of Ca^{2+} or other Ca^{2+} regulatory mechanisms. The initial rate of TG-induced Ba^{2+} entry in cells transfected with STIM1 siRNA was

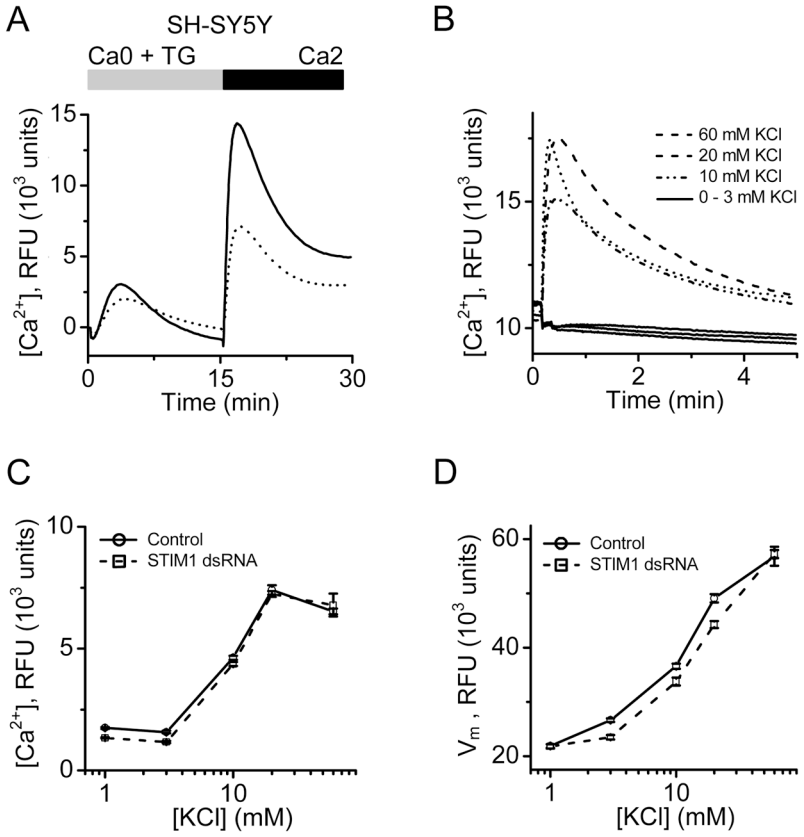

Figure 8. **Specificity of STIM1 RNAi in SH-SY5Y cells.** (A) Effects of STIM1 RNAi on SOC influx in SH-SY5Y cells. TG-dependent Ca^{2+} entry in STIM1 siRNA-treated cells (dotted line) is greatly reduced compared with control cells (solid line). Traces from cells treated with vehicle (DMSO) instead of TG were essentially flat (not depicted for clarity). (B) KCl-evoked Ca^{2+} signals as a measure of voltage-gated Ca^{2+} channel activity. Data presented as fluo-4 RFUs. At concentrations of 3 mM KCl or below, no significant change in cytosolic Ca^{2+} was observed. At 10, 20, and 60 mM KCl, a rapid rise in cytosolic Ca^{2+} was detected. (C) Maximal KCl-evoked RFU values are not different in control and STIM1-knockdown cells. (D) STIM1 suppression does not affect the resting membrane potential or the response to depolarization in SH-SY5Y cells. To monitor changes in membrane potential, a FLIPR membrane potential assay kit (Molecular Devices) was used as per the manufacturer's protocols. Data presented in RFUs. Cells were depolarized with increasing concentration of KCl, as in B. Error bars represent SD.

only 17% of control, whereas Ba^{2+} entry was unaffected in cells transfected with siRNA for STIM2 (Fig. 6 F). In contrast, stable overexpression of STIM1 in HEK293 cells modestly enhanced TG-induced Ca^{2+} entry by an average of 17% (Fig. 7 B). Interestingly, the increase in SOC influx was small in comparison to the robust increase in STIM1 protein levels (Fig. 7 A), and definitive SOC current was still not detected, nor was there any change in Mg^{2+}-inhibited cation current (Fig. 7, B–G). Thus, although STIM1 is required for SOC influx in HEK293 cells at the level of Ca^{2+} (or Ba^{2+}) entry across the plasma membrane, overexpression does not appear to greatly enhance the number of activatable SOC channels.

Effects of STIM1 protein suppression were further analyzed in SH-SY5Y cells that express voltage-gated Ca^{2+} channels (N- and L-type; Reeve et al., 1994). SOC influx in cells treated with the STIM1 siRNA was reduced to <50% of control levels (Fig. 8 A), similar to the effect observed in HEK293 cells. RNAi-mediated knockdown of STIM1 had no significant effect on the peak or kinetics of the KCl-induced Ca^{2+} signal or on the resting membrane potential of these cells (Fig. 8, B–D), indicating that knockdown of STIM1 did not have a general effect on Ca^{2+} entry mechanisms and that the effect of STIM1 knockdown on SOC influx was not due to a collapse in membrane potential. Together, these data indicate that STIM1 is required for SOC influx in mammalian cells but does not influence agonist-induced Ca^{2+} release from IP_3-sensitive stores, Ca^{2+} influx through voltage-gated Ca^{2+} channels, or the membrane potential.

Discussion

Our experiments using RNAi in conjunction with several measures of Ca^{2+} influx in intact cells indicate that STIM1 has an essential and conserved role in regulating SOC influx and CRAC channel function. Suppression of *Stim* in *Drosophila* cells, or its homologue STIM1 in three different human cell lines, inhibited TG-evoked Ca^{2+} influx, agonist-induced Ca^{2+} influx, and CRAC channel activity, but did not significantly affect resting $[Ca^{2+}]_i$ or Ca^{2+} release from intracellular stores induced by TG or by agonist stimulation. Suppression of STIM1 also had no effect on voltage-dependent Ca^{2+} entry in mammalian cells, and did not alter plasma membrane or mitochondrial membrane potentials. These data indicate that STIM1 is not a general component of Ca^{2+} influx channels, nor does it influence Ca^{2+} release from internal stores, general Ca^{2+} buffering, or the membrane potential. Although we have not examined, and do not rule out, a role for STIM1 in other forms of PLC-mediated Ca^{2+} entry, it is clear that STIM1 is required for SOC influx and CRAC channel activity in *Drosophila* and human cells.

STIM1 was originally identified in a screen for stromal cell gene products that bound to preB cells (Oritani and Kincade, 1996). This gene is conserved in sequence from *Drosophila* to mammalian species and appears to be expressed ubiquitously in human tissues, based on published analyses of mRNA and protein expression (Manji et al., 2000; Williams et al., 2001). In separate studies, STIM1, first named GOK, was proposed to suppress tumor cell growth and to affect cell morphology (Parker et al., 1996; Sabbioni et al., 1997). In our RNAi experi-

ments, we detected no changes in phenotype, growth characteristics, or cell adhesion after suppression of *Stim* in *Drosophila* S2 cells (unpublished data). Thus, we could not establish a connection between CRAC currents and tumor suppressor genes; the effects of STIM1 on cell growth may depend on cell type.

Models of STIM1 function

How might STIM1 affect SOC influx and CRAC channel function? The simplest model would have STIM1 as the sole component of the Ca^{2+} influx channel. In support of this model, our *Drosophila* genome-wide search identified numerous potential ion channel genes as well as Ca^{2+}-binding proteins with transmembrane domains, yet only *Stim* had a detectable effect on SOC influx and CRAC channel activity. However, the possibility also exists that other ion channels in *Drosophila* have novel protein domains and so eluded our bioinformatic search. Moreover, overexpression of STIM1 by nearly 100-fold in HEK293 cells enhanced SOC influx by only 17%, and did not induce detectable SOC current, arguing that STIM1 is probably not the channel itself. A second model suggests that STIM1 functions as a component that would facilitate assembly and regulate activity of SOC influx channels in different tissues, serving as an essential subunit. Mechanistically, STIM1 might function as a Ca^{2+} sensor or a coupler linking store depletion to activation of SOC influx channels. STIM1 is an abundant protein that is present on both plasma membrane and intracellular membranes (Manji et al., 2000). Its NH_2-terminal putative EF-hand Ca^{2+}-binding motif is located outside the cell and, presumably, in the lumen of the ER where it could function as a Ca^{2+} sensor. In this model, STIM1 would be an integral component of SOC influx and CRAC channel activity on the plasma membrane in addition to being present in membranes of ER Ca^{2+} stores, and homotypic association of STIM1 could play a role in linking Ca^{2+} store depletion to activation of SOC influx channels. Consistent with this model, in an initial yeast two-hybrid screen using a human thymus library, a cytoplasmic region of STIM1 itself was the strongest interactor with the intracellular coiled-coil domain of STIM1 (unpublished data), and STIM1 has been reported to homo-oligomerize (Williams et al., 2002). These data make plausible a possible STIM1–STIM1 interaction linking the cytoplasmic domains of STIM1 located at the plasma membrane with STIM1 in the ER.

Other candidate genes

Ion channels often exist in multi-subunit complexes, and regulatory functions can reside in auxiliary subunits. It is, therefore, of great interest to identify all components of store-operated channels, including the Ca^{2+}-permeable channel and components involved in the coupling of ER stores to Ca^{2+} entry. We identified two genes that, when knocked down by RNAi, resulted in an increase in the basal Ca^{2+} levels. One of these, CG2165, has homology to a plasma membrane Ca^{2+}-ATPase sequence. As would be expected, inhibiting expression of a plasma membrane Ca^{2+} pump resulted in elevation of cytosolic Ca^{2+} levels. Suppression of CG8743 also elevated intracellular Ca^{2+} levels in S2 cells, but neither CG2165 nor CG8743 detectably altered SOC influx or CRAC channel function.

RNAi targeting all three *trp* genes individually, or as a group, had no detectable effect on SOC influx. We also targeted every *trp*-related gene without altering SOC influx. Nevertheless, because we were unable to verify the effectiveness of RNAi at the protein level, we cannot conclusively exclude all *trp*s as components of *Drosophila* CRAC channels. CD20 is a tetraspanning membrane protein that has been implicated in Ca^{2+} signaling in B cells (Bubien et al., 1993; Li et al., 2003), but its expression is restricted, and there is no *Drosophila* homologue of CD20; thus, CD20 would not be expected to have a generalized role in SOC influx. Reports of nonchannel-like proteins involved in the regulation of SOC influx are now emerging. The adaptor protein Homer binds to TRPC1 and is postulated to facilitate an association with the IP_3 receptor (Yuan et al., 2003). In this case, dissociation of Homer from TRPC1 activates the TRPC1 channel. We tested the role of *Drosophila homer* (CG11324) by RNAi in S2 cells, but detected no effect on SOC influx. Another example is the inhibitor of myogenic family, isoform a (I-mfa), which is an inhibitor of MyoD and other basic helix-loop-helix transcription factors that was identified as a binding partner for TRPC1 by yeast two-hybrid studies (Ma et al., 2003). Overexpression of I-mfa inhibited store-operated currents in CHO-K1 cells that express TRPC1, whereas knockdown of I-mfa by RNAi enhanced TG-induced currents in A431 cells that also express TRPC1, suggesting I-mfa has a suppressive effect on native SOC influx mediated by TRPC1. However, we found no *Drosophila* homologue of I-mfa. A recent study demonstrated a structural role of PLCγ in calcium signaling. However, in this case suppression of endogenous PLCγ affected receptor-stimulated Ca^{2+} entry but not SOC influx activated by TG (Patterson et al., 2002). An example of indirect regulation of SOC influx has been described in which a presenilin-1 mutant associated with familial Alzheimer's disease caused overfilling of Ca^{2+} stores and a reduction in SOC influx (Leissring et al., 2000). We also targeted presenilin in *Drosophila* S2 cells, but saw no effect on SOC influx. Yet another report has implicated junctate in SOC influx and Ca^{2+} release from the ER (Treves et al., 2004). However, we found no *Drosophila* homologue for the junctate protein, so it is unlikely to play a conserved role in CRAC-mediated Ca^{2+} entry. Finally, a role has been proposed for Ca^{2+}-independent PLA_2 ($iPLA_2$) in the control of SOC influx in vascular smooth muscle cells, human platelets, human Jurkat T lymphocytes, and rat basophilic leukemia cells (Smani et al., 2003, 2004). In this case, however, $iPLA_2$ is not implicated as a structural component of either SOC influx coupling or of the plasma membrane channel complex, but rather is suggested to involve a calcium influx factor, an uncharacterized molecule hypothesized to control the activation of Ca^{2+} entry in response to discharge of Ca^{2+} stores (Randriamampita and Tsien, 1993). Many genes, including the *Drosophila* homologue of iPLA2 (CG6718), were not tested in our S2 cell screen because they did not meet our in silico search criteria. Therefore, a more extensive genome-wide screen may identify additional novel components of the SOC influx pathway.

It is, perhaps, surprising that after targeting 170 likely candidate genes the only one with a demonstrable role was

Stim. The mammalian homologue STIM1, a modular single-pass transmembrane protein with protein–protein interaction domains on both sides of the membrane, thus emerges as a central and conserved component in controlling SOC influx and CRAC channel function in *Drosophila* and human cells. STIM1 should provide a key tool in identifying the molecular mechanisms involved in CRAC channel function, activation, and Ca^{2+} signaling.

Materials and methods

Cell lines

Drosophila S2 cells (Invitrogen) used in the RNAi screen were propagated in Schneider's medium (Invitrogen) supplemented with 12.5% FBS (Invitrogen) at 22°C. *Drosophila* S2 cells used in single cell imaging and patch-clamp experiments were cultured in Schneider's *Drosophila* medium containing 10% FCS and 1% glutamine, pH 6.6, at RT in a CO_2-free incubator. HEK293 cells and Jurkat T cells (American Type Culture Collection [ATCC]) were maintained and propagated as detailed by the ATCC. SH-SY5Y cells (ATCC) were cultured as recommended by Ross et al. (1983) to maintain a neuroblastic phenotype. Cell viability was monitored with alamarBlue (Biosource International).

Preparation of dsRNA

PCR templates for dsRNA synthesis were designed to produce a 500-bp fragment with T7 and T3 RNA polymerase-binding sites on the sense and anti-sense strands, respectively. The PCR template did not need to consist entirely of exonic sequence; thus, primers containing intronic sequence could be used successfully. For PCR primer pairs, see Table S2, available at http://www.jcb.org/cgi/content/full/jcb.200502019/DC1. PCR templates were generated using Long Template PCR system (Roche). The MEGAscript T7 and T3 kits (Ambion) were used to synthesize the dsRNA as per the manufacturer's protocol. Sense and anti-sense RNA strands were annealed by heating them to 65°C for 30 min and then slowly cooling to RT.

RNAi in *Drosophila* S2 cells

RNAi experiments were adapted from the protocols described by Worby et al. (2001). *Drosophila* S2 cells (6×10^6) were seeded in T-75 flasks in 6 ml of S2 media. Cells were allowed to attach and the media was removed and replaced with 6 ml of serum-free S2 media. 30 μg dsRNA (~37 nM) was added and cells were incubated at 22°C for 30 min with gentle rocking. 12 ml of S2 media was added and cells were incubated for 5 d at 22°C. Cells were then harvested and either plated for fluorimetric analysis, single cell Ca^{2+} imaging or patch-clamp experiments, or processed for RT-PCR analysis.

RNAi in mammalian cells

siRNAs were designed according to the recommendations of Tuschl (The siRNA user guide: http://www.rockefeller.edu/labheads/tuschl/sirna.html, revised 2003) and are listed in Table S2. Initial experiments were performed with huSTIM1-1140 siRNA, and the results were confirmed with huSTIM1-1414. All subsequent experiments were performed using huSTIM1-1140. siRNAs were purchased from Dharmacon. The scrambled, nonsilencing, control siRNA was obtained from Xeragon/QIAGEN. Transfections of siRNAs into mammalian cells were performed using QIAGEN TransMessenger Transfection Reagent.

To generate the short hairpin-loop construct, hairpin-forming oligonucleotides corresponding to the STIM1-1140 siRNA (Table S2) were annealed and ligated into pSilencer 2.1-U6 neo (Ambion) according to the manufacturer's protocol. Correct inserts were verified by DNA sequencing. For the control, the Negative Control oligo (Ambion) was cloned as above.

Generation of stable cell lines

Jurkat T cells expressing a short hairpin siRNA to suppress STIM1 were prepared by electroporation using a Bio-Rad Gene Pulser. Stable pools of cells expressing functional short hairpin loop constructs were assessed by measuring levels of STIM1 protein and mRNA. To prepare HEK cell lines that overexpress STIM1, we first designed a cDNA encoding full-length human STIM1 using the strategy used by Williams et al. (2002) and cloned STIM1 into pcDNA3.1/Zeo (Invitrogen). Plasmid clone pcDNA[STIM1/542-5] was confirmed by sequencing. For cell lines stably expressing STIM1 or empty plasmid, pcDNA3.1/Zeo or pcDNA[STIM1/542-5] were transfected into HEK293 cells. Colonies of cells stably expressing STIM1 mRNA and protein were selected and then subcloned by limiting dilution.

Antibodies and Western blotting

Cell extracts were prepared by washing the cells with PBS and then extracting proteins with lysis buffer (in mM): 50 HEPES, 150 NaCl, 1.5 $MgCl_2$, 1 EDTA, 10 Na-pyrophosphate, pH 7.4, 10% glycerol, 1% Triton X-100. STIM1 pAbs (1:2,500) were generated by Alpha Diagnostic, Inc. to a COOH-terminal peptide (STIM1-CT: DNGSIGEETDSSPGRKKFPLKIFKKPLKK) as described previously (Manji et al., 2000) and were used for Western blots. Anti-GOK mAbs (1:20) were obtained from BD Biosciences and were used for immunofluorescence studies. Anti-GAPDH mAbs (1:5,000) were obtained from Research Diagnostics.

Microscopic techniques

For immunofluorescence, HEK293 cells were grown on coverslips and fixed in 4% PFA, then washed with PBS and PBS + 0.1 M glycine, and finally blocked with PBS/2% BSA/1% fish skin gelatin/15% horse serum/0.1% saponin. Fixed cells were incubated with primary antibody overnight at 4°C, and Alexa-conjugated secondary antibodies (Molecular Probes) were applied at a dilution of 1:1,000. Fluorescence images were documented using DeltaVision Deconvolution microscope (API) equipped with a Photometrics CH350L liquid cooled CCD camera attached to an inverted microscope (model IX_70; Olympus). These data were collected at RT using a 60× oil immersion objective lens (NA 1.4) and the DAPI and FITC filter sets. All images were deconvolved using constrained iterative algorithms (10 iterations) of DeltaVision software (softWoRx, v. 2.5). The deconvolved images were subsequently processed (merged and converted into tiff format) using softWoRx, v. 2.5.

Measurement of intracellular calcium with Fluo-4

Drosophila S2 cells, plated in a 96-well plate, were loaded with 10 μM fluo-4/AM (Molecular Probes) for 1 h at 22°C in buffer containing (in mM): 120 NaCl, 5 KCl, 4 $MgCl_2$, 2 $CaCl_2$, 10 Hepes, 2.5 probenecid, pH 7.2. Cells were then washed in calcium-free buffer and fluorescence levels were monitored in a FluoroSkan Ascent single-channel fluorimeter (Scientific Sales, Inc.). The single-read RNAi-based screen was based upon recording of initial fluorescence for 30 s to estimate basal Ca^{2+} levels, followed by addition of either vehicle (0.01% DMSO) or 1 μM TG (LC Labs). After a 5-min incubation, 2 mM $CaCl_2$ (final concentration) was added and cellular fluorescence was measured three min after Ca^{2+} addition as an index of SOC influx in each well. For kinetic measurements, fluorescence was recorded every 2 s throughout the entire protocol.

HEK293 cells and SH-SY5Y cells plated in 384-well plates were loaded with 5 μM fluo-4/AM in culture medium for 1 h at 25°C, then washed in calcium-free HBSS (Irvine Scientific) containing (in mM) 10 Hepes and 1 $MgCl_2$, and placed in a FLIPR^{384} fluorimeter (Molecular Devices). Cells were treated with 1 μM TG or vehicle (DMSO) for 15 min followed by addition of 1.8 mM $CaCl_2$ (final concentration). To detect the rate of Ba^{2+} entry in HEK293 cells, $BaCl_2$ (10 mM final concentration) was added instead of $CaCl_2$. To quantify the rate of cation influx, the first 30 s after cation addition was analyzed by linear regression. For agonist-induced responses in HEK293 cells, cells in calcium-free buffer were stimulated with 300 μM methylcholine for five min, followed by the addition of 1.8 mM $CaCl_2$.

Single-cell $[Ca^{2+}]_i$ imaging

Solution recipes are indicated in Table S3, available at http://www.jcb.org/cgi/content/full/jcb.200502019/DC1. After treatment with dsRNA, *Drosophila* S2 cells were loaded with fura-2 (2 μM fura-2/AM and 0.02% pluronic acid both from Molecular Probes, in S2 Ringer solution for 1 h at RT) and imaged to monitor $[Ca^{2+}]_i$ in individual cells. Jurkat T cells, both control 2A4 and STIM1-suppressed clone 4A5, were loaded with fura-2/AM (2 μM for 30 min at RT) in culture medium (RPMI, 10% FCS, 1% glucose, 600 μg/ml geneticin). S2 or Jurkat cells loaded with fura-2 were mounted in a chamber permitting solution exchange by a syringe-driven perfusion system and placed on the stage of an Axiovert 35 microscope (Carl Zeiss MicroImaging, Inc.) equipped with a 40× plan-Neofluar objective (NA 1.30 oil). Alternating 340 ± 5 or 380 ± 5 nm light controlled by a high speed wavelength switcher (Lambda DG-4; Sutter Instrument Co.), was used to excite fura-2. A 400-nm dichroic mirror and 480-nm long-pass emission filter (Chroma) supplied light to the Photometrics CoolSNAP HQ CCD camera (Roper Scientific), and images were acquired under control of Metafluor software (Universal Imaging Corp.). $[Ca^{2+}]_i$ was estimated using the formula $[Ca^{2+}]_i = K\,(R - R_{min})/(R_{max} - R)$.

The values of R_{min} and R_{max} were determined in intact cells by exposing cells to Ca^{2+}-free solution containing 1 μM ionomycin (Calbiochem) to obtain R_{min}, and 10 mM Ca^{2+} solution with 1 μM ionomycin to obtain R_{max}. $[Ca^{2+}]_i$ was then calculated using an effective K value for fura-2 of 248 nM, as determined previously (Fanger et al., 2000).

Whole-cell recording

Patch-clamp experiments were performed at RT in the standard whole-cell recording configuration, as described previously (Yeromin et al., 2004). External and internal solutions are indicated in Table S3. S2, Jurkat, or HEK cells were initially bathed in the appropriate external solution. After gigohm seal formation, whole-cell recording was initiated at time 0. The membrane potential was held at 10 mV. Voltage ramps from −110 mV to +110 mV lasting 220 ms were alternated with 220-ms pulses to −110 mV every 2. Up to eight I-V curves were averaged for display. Leak currents before channel activation were averaged (up to five sweeps) and subtracted from subsequent current records. External solutions were changed locally by fast application using a gravity-driven perfusion system. A complete local solution exchange was achieved within 2 s. Data were analyzed using Pulse (Heka Electronic) and Origin (OriginLab Corp.). The membrane capacitance (a measure of cell surface area) of S2 cells selected for recording was 11.3 ± 0.5 pF (mean ± SEM, n = 211 cells); for Jurkat T cells the capacitance was 12.5 ± 1.1 pF (n = 25). To calculate current densities, peak current amplitudes were divided by membrane capacitance for each cell.

Online supplemental material

Table S1 lists all the candidate genes that were targeted in the RNAi-based screen for components of the SOC influx pathway in S2 cells. Included in Table S1 is a description of the strategies used to compile the final list of candidate genes, and whether mRNA for the individual genes was detected by RT-PCR. Table S2 lists primer sequences used for preparing dsRNAs, shRNAs, and PCR reactions, as well as sequences used for siRNAs. Table S3 shows the composition of solutions used for Ca^{2+} imaging and whole-cell recordings. Online supplemental material is available at http://www.jcb.org/cgi/content/full/jcb.200502019/DC1.

We thank Dr. Craig Montell for bringing to our attention the utility of RNAi in S2 cells. We thank Lara Marlin and John Vekich for excellent technical assistance, Sindy Wei for help with $[Ca^{2+}]_i$ imaging, and Dr. Luette Forrest for help with cell culture.

A.V. Yeromin, M. Lioudyno, O. Safrina, S. Zjang, J.A. Kozak, and M.D. Cahalan were supported by National Institutes of Health grant NS14609. This work was supported in part by a UC/Industry Discovery grant 01-10139.

Submitted: 4 February 2005
Accepted: 23 March 2005

References

Bubien, J.K., L.J. Zhou, P.D. Bell, R.A. Frizzell, and T.F. Tedder. 1993. Transfection of the CD20 cell surface molecule into ectopic cell types generates a Ca^{2+} conductance found constitutively in B lymphocytes. *J. Cell Biol.* 121:1121–1132.

Clapham, D.E. 2003. TRP channels as cellular sensors. *Nature.* 426:517–524.

Clemens, J.C., C.A. Worby, N. Simonson-Leff, M. Muda, T. Maehama, B.A. Hemmings, and J.E. Dixon. 2000. Use of double-stranded RNA interference in *Drosophila* cell lines to dissect signal transduction pathways. *Proc. Natl. Acad. Sci. USA.* 97:6499–6503.

Cui, J., J.S. Bian, A. Kagan, and T.V. McDonald. 2002. CaT1 contributes to the store-operated calcium current in Jurkat T-lymphocytes. *J. Biol. Chem.* 277:47175–47183.

Fagan, K.A., K.E. Smith, and D.M. Cooper. 2000. Regulation of the Ca^{2+}-inhibitable adenylyl cyclase type VI by capacitative Ca^{2+} entry requires localization in cholesterol-rich domains. *J. Biol. Chem.* 275:26530–26537.

Fanger, C.M., A.L. Neben, and M.D. Cahalan. 2000. Differential Ca^{2+} influx, KCa channel activity, and Ca^{2+} clearance distinguish Th1 and Th2 lymphocytes. *J. Immunol.* 164:1153–1160.

Kahr, H., R. Schindl, R. Fritsch, B. Heinze, M. Hofbauer, M.E. Hack, M.A. Mortelmaier, K. Groschner, J.B. Peng, H. Takanaga, et al. 2004. CaT1 knock-down strategies fail to affect CRAC channels in mucosal-type mast cells. *J. Physiol.* 557:121–132.

Leissring, M.A., Y. Akbari, C.M. Fanger, M.D. Cahalan, M.P. Mattson, and F.M. LaFerla. 2000. Capacitative calcium entry deficits and elevated luminal calcium content in mutant presenilin-1 knockin mice. *J. Cell Biol.* 149:793–798.

Lewis, R.S. 2001. Calcium signaling mechanisms in T lymphocytes. *Annu. Rev. Immunol.* 19:497–521.

Li, H., L.M. Ayer, J. Lytton, and J.P. Deans. 2003. Store-operated cation entry mediated by CD20 in membrane rafts. *J. Biol. Chem.* 278:42427–42434.

Ma, R., D. Rundle, J. Jacks, M. Koch, T. Downs, and L. Tsiokas. 2003. Inhibitor of myogenic family, a novel suppressor of store-operated currents through an interaction with TRPC1. *J. Biol. Chem.* 278:52763–52772.

Magyar, A., and A. Varadi. 1990. Molecular cloning and chromosomal localization of a sarco/endoplasmic reticulum-type $Ca^{2(+)}$-ATPase of *Drosophila melanogaster*. *Biochem. Biophys. Res. Commun.* 173:872–877.

Manji, S.S., N.J. Parker, R.T. Williams, L. van Stekelenburg, R.B. Pearson, M. Dziadek, and P.J. Smith. 2000. STIM1: a novel phosphoprotein located at the cell surface. *Biochim. Biophys. Acta.* 1481:147–155.

Montell, C. 2003. The venerable inveterate invertebrate TRP channels. *Cell Calcium.* 33:409–417.

Mori, Y., M. Wakamori, T. Miyakawa, M. Hermosura, Y. Hara, M. Nishida, K. Hirose, A. Mizushima, M. Kurosaki, E. Mori, et al. 2002. Transient receptor potential 1 regulates capacitative Ca^{2+} entry and Ca^{2+} release from endoplasmic reticulum in B lymphocytes. *J. Exp. Med.* 195:673–681.

Oritani, K., and P.W. Kincade. 1996. Identification of stromal cell products that interact with pre-B cells. *J. Cell Biol.* 134:771–782.

Parker, N.J., C.G. Begley, P.J. Smith, and R.M. Fox. 1996. Molecular cloning of a novel human gene (D11S4896E) at chromosomal region 11p15.5. *Genomics.* 37:253–256.

Patterson, R.L., D.B. van Rossum, D.L. Ford, K.J. Hurt, S.S. Bae, P.G. Suh, T. Kurosaki, S.H. Snyder, and D.L. Gill. 2002. Phospholipase C-gamma is required for agonist-induced Ca^{2+} entry. *Cell.* 111:529–541.

Philipp, S., C. Trost, J. Warnat, J. Rautmann, N. Himmerkus, G. Schroth, O. Kretz, W. Nastainczyk, A. Cavalie, M. Hoth, and V. Flockerzi. 2000. TRP4 (CCE1) protein is part of native calcium release-activated Ca^{2+}-like channels in adrenal cells. *J. Biol. Chem.* 275:23965–23972.

Philipp, S., B. Strauss, D. Hirnet, U. Wissenbach, L. Mery, V. Flockerzi, and M. Hoth. 2003. TRPC3 mediates T-cell receptor-dependent calcium entry in human T-lymphocytes. *J. Biol. Chem.* 278:26629–26638.

Prakriya, M., and R.S. Lewis. 2003. CRAC channels: activation, permeation, and the search for a molecular identity. *Cell Calcium.* 33:311–321.

Putney, J.W., Jr., and G.S. Bird. 1993. The signal for capacitative calcium entry. *Cell.* 75:199–201.

Randriamampita, C., and R.Y. Tsien. 1993. Emptying of intracellular Ca^{2+} stores releases a novel small messenger that stimulates Ca^{2+} influx. *Nature.* 364:809–814.

Reeve, H.L., P.F. Vaughan, and C. Peers. 1994. Calcium channel currents in undifferentiated human neuroblastoma (SH-SY5Y) cells: actions and possible interactions of dihydropyridines and omega-conotoxin. *Eur. J. Neurosci.* 6:943–952.

Ross, R.A., B.A. Spengler, and J.L. Biedler. 1983. Coordinate morphological and biochemical interconversion of human neuroblastoma cells. *J. Natl. Cancer Inst.* 71:741–747.

Sabbioni, S., G. Barbanti-Brodano, C.M. Croce, and M. Negrini. 1997. GOK: a gene at 11p15 involved in rhabdomyosarcoma and rhabdoid tumor development. *Cancer Res.* 57:4493–4497.

Schindl, R., H. Kahr, I. Graz, K. Groschner, and C. Romanin. 2002. Store depletion-activated CaT1 currents in rat basophilic leukemia mast cells are inhibited by 2-aminoethoxydiphenyl borate. Evidence for a regulatory component that controls activation of both CaT1 and CRAC ($Ca^{(2+)}$ release-activated $Ca^{(2+)}$ channel) channels. *J. Biol. Chem.* 277:26950–26958.

Smani, T., S.I. Zakharov, E. Leno, P. Csutora, E.S. Trepakova, and V.M. Bolotina. 2003. Ca^{2+}-independent phospholipase A2 is a novel determinant of store-operated Ca^{2+} entry. *J. Biol. Chem.* 278:11909–11915.

Smani, T., S.I. Zakharov, P. Csutora, E. Leno, E.S. Trepakova, and V.M. Bolotina. 2004. A novel mechanism for the store-operated calcium influx pathway. *Nat. Cell Biol.* 6:113–120.

Tiruppathi, C., M. Freichel, S.M. Vogel, B.C. Paria, D. Mehta, V. Flockerzi, and A.B. Malik. 2002. Impairment of store-operated Ca^{2+} entry in $TRPC4^{-/-}$ mice interferes with increase in lung microvascular permeability. *Circ. Res.* 91:70–76.

Towers, P.R., and D.B. Sattelle. 2002. A *Drosophila melanogaster* cell line (S2) facilitates post-genome functional analysis of receptors and ion channels. *Bioessays.* 24:1066–1073.

Trebak, M., G.S. Bird, R.R. McKay, and J.W. Putney Jr. 2002. Comparison of human TRPC3 channels in receptor-activated and store-operated modes. Differential sensitivity to channel blockers suggests fundamental differences in channel composition. *J. Biol. Chem.* 277:21617–21623.

Treves, S., C. Franzini-Armstrong, L. Moccagatta, C. Arnoult, C. Grasso, A.

Schrum, S. Ducreux, M.X. Zhu, K. Mikoshiba, T. Girard, et al. 2004. Junctate is a key element in calcium entry induced by activation of $InsP_3$ receptors and/or calcium store depletion. *J. Cell Biol.* 166:537–548.

Vazquez-Martinez, O., R. Canedo-Merino, M. Diaz-Munoz, and J.R. Riesgo-Escovar. 2003. Biochemical characterization, distribution and phylogenetic analysis of *Drosophila melanogaster* ryanodine and IP_3 receptors, and thapsigargin-sensitive Ca^{2+} ATPase. *J. Cell Sci.* 116:2483–2494.

Venkatachalam, K., D.B. van Rossum, R.L. Patterson, H.T. Ma, and D.L. Gill. 2002. The cellular and molecular basis of store-operated calcium entry. *Nat. Cell Biol.* 4:E263–E272.

Voets, T., J. Prenen, A. Fleig, R. Vennekens, H. Watanabe, J.G. Hoenderop, R.J. Bindels, G. Droogmans, R. Penner, and B. Nilius. 2001. CaT1 and the calcium release-activated calcium channel manifest distinct pore properties. *J. Biol. Chem.* 276:47767–47770.

Williams, R.T., S.S. Manji, N.J. Parker, M.S. Hancock, L. Van Stekelenburg, J.P. Eid, P.V. Senior, J.S. Kazenwadel, T. Shandala, R. Saint, et al. 2001. Identification and characterization of the STIM (stromal interaction molecule) gene family: coding for a novel class of transmembrane proteins. *Biochem. J.* 357:673–685.

Williams, R.T., P.V. Senior, L. Van Stekelenburg, J.E. Layton, P.J. Smith, and M.A. Dziadek. 2002. Stromal interaction molecule 1 (STIM1), a transmembrane protein with growth suppressor activity, contains an extracellular SAM domain modified by N-linked glycosylation. *Biochim. Biophys. Acta.* 1596:131–137.

Winslow, M.M., J.R. Neilson, and G.R. Crabtree. 2003. Calcium signalling in lymphocytes. *Curr. Opin. Immunol.* 15:299–307.

Worby, C.A., N. Simonson-Leff, and J.E. Dixon. 2001. RNA interference of gene expression (RNAi) in cultured *Drosophila* cells. *Sci. STKE.* 2001:PL1.

Wu, X., G. Babnigg, and M.L. Villereal. 2000. Functional significance of human trp1 and trp3 in store-operated $Ca^{(2+)}$ entry in HEK-293 cells. *Am. J. Physiol. Cell Physiol.* 278:C526–C536.

Yagodin, S., N.B. Pivovarova, S.B. Andrews, and D.B. Sattelle. 1999. Functional characterization of thapsigargin and agonist-insensitive acidic Ca^{2+} stores in *Drosophila melanogaster* S2 cell lines. *Cell Calcium.* 25:429–438.

Yeromin, A.V., J. Roos, K.A. Stauderman, and M.D. Cahalan. 2004. A store-operated calcium channel in *Drosophila* S2 cells. *J. Gen. Physiol.* 123:167–182.

Yuan, J.P., K. Kiselyov, D.M. Shin, J. Chen, N. Shcheynikov, S.H. Kang, M.H. Dehoff, M.K. Schwarz, P.H. Seeburg, S. Muallem, and P.F. Worley. 2003. Homer binds TRPC family channels and is required for gating of TRPC1 by IP_3 receptors. *Cell.* 114:777–789.

Yue, L., J.B. Peng, M.A. Hediger, and D.E. Clapham. 2001. CaT1 manifests the pore properties of the calcium-release-activated calcium channel. *Nature.* 410:705–709.